Neuroscience 130 (2005) 165–183

INDIRECT PROJECTIONS FROM THE SUPRACHIASMATIC NUCLEUS TO MAJOR AROUSAL-PROMOTING CELL GROUPS IN RAT: IMPLICATIONS FOR THE CIRCADIAN CONTROL OF BEHAVIOURAL STATE

S. DEURVEILHER AND K. SEMBA*

Department of Anatomy and Neurobiology, Faculty of Medicine, Dalhousie University, 5850 College Street, Halifax, Nova Scotia, Canada B3H 1X5

Abstract—The circadian clock housed in the suprachiasmatic nucleus (SCN) controls various circadian rhythms including daily sleep–wake cycles. Using dual tract-tracing, we recently showed that the medial preoptic area (MPA), subparaventricular zone (SPVZ) and dorsomedial hypothalamic nucleus (DMH) are well positioned to relay SCN output to two key sleep-promoting nuclei, namely, the ventrolateral and median preoptic nuclei. The present study examined the possibility that these three nuclei may link the SCN with wake-regulatory neuronal groups. Biotinylated dextran-amine with or without cholera toxin B subunit was injected into selected main targets of SCN efferents; the retrograde labeling in the SCN was previously analyzed. Here, anterograde labeling was analyzed in immunohistochemically identified cholinergic, orexin/hypocretin-containing and aminergic cell groups. Tracer injections into the MPA, SPVZ and DMH resulted in moderate to dense anterograde labeling of varicose fibers in the orexin field and the tuberomammillary nucleus. The locus coeruleus, particularly the dendritic field, contained moderate anterograde labeling from the MPA and DMH. The ventral tegmental area, dorsal raphe nucleus, and laterodorsal tegmental nucleus all showed moderate anterograde labeling from the DMH. The substantia innominata showed moderate anterograde labeling from the MPA. These results suggest that the MPA, SPVZ and DMH are possible relay nuclei for indirect SCN projections not only to sleep-promoting preoptic nuclei as previously shown, but also to wake-regulatory cell groups throughout the brain. In the absence of major direct SCN projections to most of these sleep/wake-regulatory regions, indirect neuronal pathways probably play an important role in the circadian control of sleep–wake cycles and other physiological functions.

Key words: dual tract-tracing, immunohistochemistry, cholinergic, orexin/hypocretin, aminergic.

*Corresponding author. Tel: +1-902-494-2008; fax: +1-902-494-1212.
E-mail address: semba@dal.ca (K. Semba).

Abbreviations: A, anterior; BDA, biotinylated dextran-amine; CTB, cholera toxin B subunit; DAB, diaminobenzidine; DMH, dorsomedial hypothalamic nucleus; HDB, horizontal limb of the diagonal band of Broca; HDC, histidine decarboxylase; ir, immunoreactive; LD, light–dark; MPA, medial preoptic area; MS-VDB, medial septum-vertical limb of the diagonal band complex; NPY, neuropeptide Y; P, posterior; PH, posterior hypothalamic area; REM, rapid eye-movement; SCN, suprachiasmatic nucleus; SPVZ, subparaventricular zone; TH, tyrosine hydroxylase; VAChT, vesicular acetylcholine transporter.

The circadian clock housed in the suprachiasmatic nucleus (SCN) of the hypothalamus governs daily rhythms of sleep–waking and other behavioral and physiological functions (Rusak and Zucker, 1979; Moore and Leak, 2001). SCN lesions in rodents abolish daily sleep–wake rhythms; interestingly, however, the amounts of sleep or wakefulness are not affected (Ibuka et al., 1977; Wurts and Edgar, 2000). These findings suggest that the SCN is not responsible for maintaining behavioral states, but influences their timing in a circadian manner. Behavioral states are, in fact, controlled by a neural system that networks across widely distributed brain regions (Steriade and McCarley, 1990; Lydic and Baghdoyan, 1999). Some of the circadian influence on the sleep/wake-regulatory system is likely to be mediated by humoral factors (LeSauter and Silver, 1998; Kramer et al., 2001; Cheng et al., 2002). However, "hard-wired" synaptic pathways certainly play a role as well (Swanson, 1987; Buijs and Kalsbeek, 2001; Pace-Schott and Hobson, 2002), and little is known about these pathways.

Following the general organizational principle of the hypothalamus (Swanson, 1987), the SCN does not project abundantly beyond the hypothalamus (Watts et al., 1987). No region in the sleep–wake regulatory system receives direct projections from the SCN, with the exception of the medial preoptic area (MPA), which receives strong direct SCN projections (Watts et al., 1987; Leak and Moore, 2001), as well as the ventrolateral preoptic nucleus (Novak and Nunez, 2000; Chou et al., 2002) and the area containing orexin (also known as hypocretin)-containing neurons in the posterior hypothalamus (Abrahamson et al., 2000), which both receive sparse direct SCN projections. Indirect pathways are certainly conceivable, however, and we have recently shown, using a dual tract-tracing method, that several known targets of direct SCN projections are well placed to relay SCN output to the ventrolateral (Deurveilher et al., 2002) and median preoptic nuclei (Deurveilher and Semba, 2003), two key structures involved in the generation of sleep (McGinty and Szymusiak, 2001; Saper et al., 2001). These potential relay nuclei are the MPA, subparaventricular zone (SPVZ), and dorsomedial hypothalamic nucleus (DMH). The synaptic connections that form the relays in each of these nuclei remain to be investigated. However, in the absence of major direct projections to the sleep–wake regulatory system, these potential indirect pathways may play an important role in circadian regulation of sleep.

0306-4522/05$30.00+0.00 © 2004 IBRO. Published by Elsevier Ltd. All rights reserved.
doi:10.1016/j.neuroscience.2004.08.030

In the present study, using the same dual tract-tracing approach, we investigated whether the previously identified potential relay nuclei to the ventrolateral and median preoptic nuclei may also relay SCN output to major arousal/wake-promoting neuronal groups, including cholinergic neurons in the basal forebrain and mesopontine tegmentum; orexin-containing neurons in the posterior hypothalamus; and aminergic neurons in the tuberomammillary nucleus, ventral tegmental area, substantia nigra pars compacta, dorsal raphe nucleus and locus coeruleus. All of these neuronal populations are thought to play important roles in the control of cortical and behavioral arousal, and some are also implicated in the mechanisms of rapid eye-movement (REM) sleep (see above). The density of anterogradely labeled varicose fibers was analyzed in each of these wake-promoting structures. Preliminary results have been reported in abstract form (Deurveilher et al., 2001a,b,c).

EXPERIMENTAL PROCEDURES

As a follow up to two previous studies from our laboratory (Deurveilher et al., 2002; Deurveilher and Semba, 2003), we performed additional histological processing of brain sections from the animals used in these previous studies. The details of animals used, tracer injections, perfusion, and immunohistochemical procedures were described in Deurveilher et al. (2002). Briefly, adult male Wistar rats were injected, under anesthesia (60 mg/kg ketamine, 3.2 mg/kg xylazine, and 0.6 mg/kg acepromazine, i.m.), with a mixture of biotinylated dextran-amine (BDA; 10% in saline) and cholera toxin subunit B (CTB; 0.25 or 0.5%), or BDA alone (10%), into the MPA (n=10), SPVZ (n=11), DMH (n=8), or posterior hypothalamic area (PH; n=7). Postinjection survival periods ranged from 8 to 11 days (mostly either 9 or 11 days) after co-injections of BDA and CTB, and from 4 to 10 days (mostly either 5 or 6 days) after single injections of BDA. No obvious differences were noted among the cases with different survival periods. All experiments were performed in compliance with the guidelines established by the Canadian Council on Animal Care and by the Dalhousie University Committee on Laboratory Animals. All efforts were made to minimize the number of animals used and their suffering.

The injection sites and the retrograde labeling in the SCN in relation to the vasopressin-rich shell, and neuropeptide Y (NPY)-rich core regions have been reported previously in detail (Deurveilher et al., 2002). For convenience, some of these results are included in the present study, with reference to the original source.

To examine anterograde BDA labeling in the wake-regulatory structures, a series of 40-μm coronal sections from each case was reacted with a standard avidin–biotin–horseradish peroxidase complex method, using diaminobenzidine (DAB) and nickel ammonium sulfate to produce a black–purple reaction product (Deurveilher et al., 2002). These sections were then reacted immunohistochemically with a peroxidase anti-peroxidase method and DAB without nickel to produce a brown reaction product. The following primary antibodies were used: rabbit anti-preprohypocretin antibody (1:1000; Chemicon International, Temecula, CA, USA) to visualize orexin/hypocretin-containing neurons in the posterior hypothalamus; rabbit anti-histidine decarboxylase [HDC; 1:1600; kindly provided by Dr. N. Inagaki, Osaka University, Osaka, Japan] to visualize histaminergic neurons in the tuberomammillary nucleus; rabbit anti-tyrosine hydroxylase (TH; 1:6000; Pel-Freez, Rogers, AR, USA) to visualize dopaminergic neurons in the ventral tegmental area and substantia nigra pars compacta, and noradrenergic neurons in the locus coeruleus; rabbit anti-serotonin (1:20,000; Diasorin, Stillwater, MN, USA) to visualize serotoninergic neurons in the dorsal raphe nucleus; and rat anti-choline acetyltransferase (1:50; Boehringer, Laval, Quebec, Canada) or rabbit anti-vesicular acetylcholine transporter (VAChT; 1:15,000; Chemicon International) to visualize cholinergic neurons in the basal forebrain [the medial septum–vertical limb of the diagonal band complex (MS-VDB), horizontal limb of the diagonal band of Broca (HDB), magnocellular preoptic nucleus, and substantia innominata] and in the mesopontine tegmentum (the pedunculopontine and laterodorsal tegmental nuclei).

In addition to the sections processed for double labeling as above, a second series of sections was reacted to visualize BDA singly for quantitative analysis of anterograde labeling in the areas mentioned above.

Data analysis

The density of anterograde labeling in the wake-related cell groups was assessed using either two or three sections for each cell group at the following anterior (A) to posterior (P) levels (mm to bregma) according to the brain atlas by Paxinos and Watson (1998): MS-VDB (A 0.7 and A 0.2); HDB (A 0.1 and P 0.3); magnocellular preoptic nucleus (P 0.3 and P 0.8); substantia innominata (P 1.3 and P 1.6); orexin cell group (P 2.8 and P 3.14); tuberomammillary nucleus (dorsal division: P 3.8 and P 4.16; ventral division: P 4.16 and P 4.3); ventral tegmental area (P 5.3 and P 5.6) and substantia nigra pars compacta (P 5.8 and P 6.04); dorsal raphe nucleus (P 7.8, P 8.2 and P 8.8); pedunculopontine (P 7.64 and P 8.3) and laterodorsal tegmental nuclei (P 8.8 and P 9.16); and locus coeruleus (dendritic region: P 9.16 and P 9.68; cell body region: P 9.68 and P 10.64). Note that the dendritic region of the locus coeruleus, which was delineated by a dense plexus of TH-immunoreactive (-ir) dendrites, overlaps with Barrington's nucleus at P 9.16 (Rizvi et al., 1994; Steininger et al., 2001). In addition to the above regions, the density of anterograde labeling was evaluated in regions of the mesencephalic reticular formation (P 6.72 and P 7.04), involved in arousal, and the pontine reticular formation (P 8.8 and P 9.3), involved in REM sleep generation (Steriade and McCarley, 1990).

As in our previous studies (Deurveilher et al., 2002; Deurveilher and Semba, 2003), anterograde labeling was analyzed using sections stained only for BDA, because the additional immunostaining often interfered with the evaluation of BDA-labeled elements. Transmitter-specific cell groups in BDA-labeled sections were identified by comparing with adjacent sections double-stained for BDA and a relevant transmitter marker. The density of anterograde labeling was assessed within a region that closely outlined the entire cluster of immunolabeled cell bodies and proximal dendrites for all the cell groups except the locus coeruleus, basal forebrain regions, orexin field, and mesencephalic and pontine reticular formation. For the locus coeruleus, dendritic and cell body regions were analyzed separately as the density of anterograde labeling appeared denser in the dendritic, than the cell body, region. For the three basal forebrain regions, the orexin field, and the mesencephalic and pontine reticular formation, density analysis boxes were used. For the MS-VDB, a box (0.4 mm in width×1.5 mm in height at A 0.7; 0.4 mm×2.5 mm at A 0.2) was placed so that its medial border was aligned with the midline of the brain section. For the HDB, a box (1 mm×0.4 mm) was positioned tangential to the ventral surface of the brain. For the substantia innominata, a box (1 mm×0.6 mm) was placed subjacent to the globus pallidus; no box was required for the magnocellular preoptic nucleus, which can be delineated easily in sections single-stained for BDA on the basis of a faint non-specific staining of its magnocellular neurons. For the orexin cell group, a box (1 mm×0.5 mm) was placed so that the midpoint of its ventral segment was centered at the fornix, thus encompassing the perifornical area where orexin neurons are most concentrated; the analysis box was then divided into two halves to analyze the medial and lateral portions separately, as anterograde labeling

appeared denser in the medial, than the lateral, portion. For the mesencephalic reticular formation, a box (1.5 mm×1 mm) was placed over the deep mesencephalic nucleus. For the pontine reticular formation, a box (1.5 mm×1 mm) was placed over the ventral part of either the rostral or caudal pontine reticular field where microinjection of cholinergic agonist can increase the amount of REM sleep in rat (Deurveilher et al., 1997). Due to the predominantly ipsilateral nature of all the staining, data analyses were conducted ipsilaterally to the injection site.

The density of varicose fibers in each wake-regulatory cell group was assessed by using the same density scale template as in our previous study (Deurveilher and Semba, 2003): absent (−), low (+), moderate (++), and dense (+++; Fig. 1). The densities from either two or three sections in each animal were averaged for each structure because, in general, there were no obvious rostrocaudal differences in density. For consistency, all analyses were conducted by the same examiner (S.D.). Digitized images of selected sections were captured with an AxioCam video camera (Zeiss), and the brightness, contrast and sharpness were adjusted for presentation. Table 1 lists the abbreviations used in Figs. 2–4 and Tables 2–5.

RESULTS

The present results were derived from the 36 rats described in Deurveilher et al. (2002) and Deurveilher and Semba (2003). Twenty-seven rats received co-injections of BDA and CTB, and nine received single injections of BDA, into one of the three main target nuclei of the SCN projections, namely the MPA, SPVZ, and DMH, as well as into the PH. Tables 2–5 show the results of all these cases, including the injection sites, and the quantitative analysis of retrograde labeling in the SCN primarily based on CTB labeling, as adapted from one of our previous studies (Deurveilher et al., 2002). The 36 cases were categorized into four groups based on the injection site: MPA (n=10); SPVZ (n=11); DMH (n=8); and PH (n=7; Deurveilher et al., 2002).

Candidates for relay nuclei that link the SCN with wake-regulatory neuronal groups were identified by the presence of both strong retrograde labeling in the SCN, and strong anterograde labeling in the wake-regulatory groups. Quantitative criteria for the strong labeling were established as follows, based on the results of the 36 cases (Deurveilher et al., 2001a,b,c, 2002; Deurveilher and Semba, 2003), as well as previous studies by others on the efferent projections of the SCN (Watts and Swanson, 1987; Leak and Moore, 2001): >20 CTB-labeled or >5 BDA-labeled neurons in the SCN per section, and at least moderate BDA-labeled varicose fibers in a given wake-regulatory cell group, for cases with medium to large injection sites; >5 CTB-labeled or >2 BDA-labeled neurons in the SCN per section, and at least low-moderate BDA-labeled varicose fibers in a given wake-regulatory cell group, for cases with small injection sites. The results reported below highlight the cases with the highest numbers of retrogradely labeled neurons in the SCN; the cases that yielded few or no retrogradely labeled neurons are mentioned as supplementary data.

The MPA

The retrograde labeling in the SCN was examined with respect to the two anatomical compartments of the SCN: the shell, as defined by the presence of vasopressin-containing neurons, and the core, as defined by the presence of NPY-containing fibers (Deurveilher et al., 2002). The retrograde CTB labeling following MPA injections indicated that the SCN projections to the MPA arose predominantly from the shell, with a small contribution from the core (Table 2). Strong retrograde labeling was also

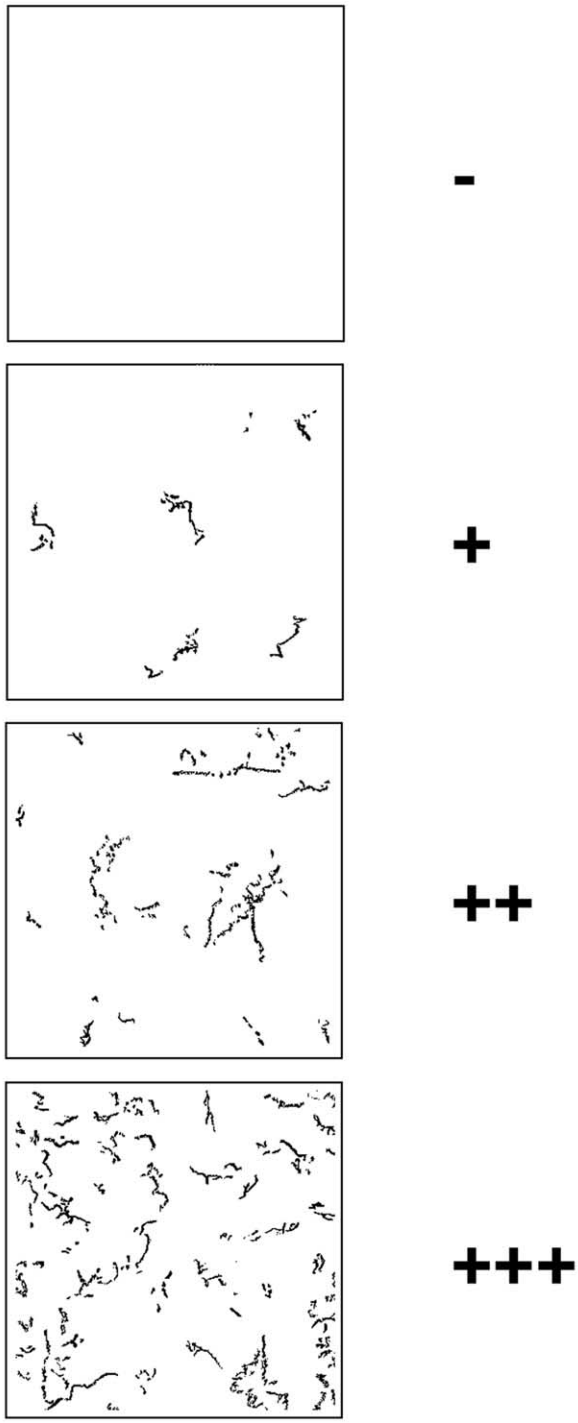

Fig. 1. The density-scale template used for assessing the density of anterograde labeling. Density: absent (−), low (+), moderate (++) and dense (+++). Semi-levels were also used as required.

Table 1. Anatomical abbreviations used in figures and Tables 2–5

3V	Third ventricle
4V	Fourth ventricle
AH	Anterior hypothalamic area
AM	Anteromedial thalamic nucleus
Bar	Barrington's nucleus
BST	Bed nucleus of the stria terminalis
CM	Central medial thalamic nucleus
DA	Dorsal hypothalamic area
DMH	Dorsomedial hypothalamic nucleus
DRN	Dorsal raphe nucleus
fx	Fornix
GP	Globus pallidus
LCc	Locus coeruleus, core or nuclear region
LCd	Locus coeruleus, dendritic region
LDT	Laterodorsal tegmental nucleus
LS	Lateral septum
me5	Mesencephalic trigeminal tract
MnPO	Median preoptic nucleus
MPA	Medial preoptic area
opt	Optic tract
ox	Optic chiasm
PeF	Perifornical area
PH	Posterior hypothalamic area
PVH	Paraventricular hypothalamic nucleus
RCh	Retrochiasmatic area
Re	Reuniens thalamic nucleus
SCN	Suprachiasmatic nucleus
scp	Superior cerebellar peduncle
SI	Substantia innominata
SP	Subparafascicular thalamic nucleus
SPVZ	Subparaventricular zone
TMNd	Tuberomammillary nucleus, dorsal part
VLPO	Ventrolateral preoptic nucleus
VMH	Ventromedial hypothalamic nucleus
VTA	Ventral tegmental area

observed in the ventral lateral septum, bed nucleus of the stria terminalis, ventromedial hypothalamic and arcuate nuclei, and the amygdala (Deurveilher et al., 2002).

The anterograde BDA labeling was analyzed in six cases for both forebrain and brainstem, and in four cases for forebrain only (Table 2). Of these 10 cases, six with the highest numbers of retrogradely labeled neurons in the SCN are described in detail below. An example of retrogradely labeled neurons in the SCN following a large injection in the MPA is shown in Fig. 2A (case 482).

Anterograde labeling in the cholinergic cell regions. As shown in Table 2, of the six injections in the MPA that produced strong retrograde labeling in the SCN, four rostral injections (472, 473, 481 and 482) produced denser labeling of varicose axons in the substantia innominata (moderate to moderate-dense; Fig. 2B) than in the other three basal forebrain regions examined (mostly sparse). Two caudal MPA injections (501 and 503) yielded sparse to low density labeling across all the basal forebrain regions.

Four MPA cases provided data primarily based on BDA labeling (406, 407, 453 and 504). As BDA is primarily an anterograde tracer, these cases showed little or no retrograde labeling in the SCN, but the anterograde labeling data were consistent with the above. Specifically, one injection in the rostral MPA (504) resulted in greater anterograde labeling in the substantia innominata than did another, caudal MPA injection (453). A third injection which was centered dorsally in the MPA yielded anterograde labeling in the MS-VDB and, to a lesser degree, in the more caudal basal forebrain cholinergic regions (406). Finally, a small injection that was centered in the bed nucleus of the stria terminalis, thus largely missing the MPA, yielded little anterograde labeling in any basal forebrain region (407).

In the brainstem, only sparse or no anterogradely labeled fibers were seen in the pedunculopontine or the laterodorsal tegmental nucleus in all the MPA cases.

Anterograde labeling in the orexin cell region. In all the six cases with strong retrograde labeling in the SCN (472, 473, 481, 482, 501 and 503), BDA-labeled varicose fibers were denser in the medial (moderate-dense to dense), than the lateral (low to moderate), part of the orexin cell field (Table 2). Many varicose fibers were seen near the orexin-ir cell bodies or proximal dendrites (Fig. 2C).

Of the two MPA injections that resulted in only a few retrogradely labeled neurons in the SCN, one injection (504) produced greater labeling in the medial, than the lateral, part of the orexin field, consistent with the preferential distribution of termination described above; the second, caudal injection (453) yielded virtually no labeling in this region.

Anterograde labeling in the aminergic cell regions. In the six cases of MPA injections yielding strong retrograde labeling in the SCN (472, 473, 481, 482, 501 and 503), moderate anterograde labeling was seen in the dorsal tuberomammillary nucleus, and slightly lighter labeling in the ventral tuberomammillary nucleus (Table 2). In the dorsal tuberomammillary nucleus, many labeled varicosities were found near HDC-ir perikarya (Fig. 2D). The anterograde labeling in the ventral tegmental area and substantia nigra pars compacta was sparse to low. The dorsal raphe nucleus contained low to moderate labeling. Moderate to dense labeling was found in the dendritic region of the locus coeruleus (the dendritic region also overlaps with Barrington's nucleus), with many labeled fibers intermingled with TH-positive dendrites. Only low to low-moderate labeling was seen in the cell body region of the locus coeruleus.

Of the two MPA injections resulting in light retrograde labeling in the SCN, the rostral injection (504) showed denser labeling in the dorsal and ventral tuberomammillary nuclei and in the dendritic region of the locus coeruleus, than in the other regions examined (Table 2); this is consistent with the above results. With the caudal injection of the two (453), the dorsal tuberomammillary nucleus contained the densest of all the anterograde labeling.

Anterograde labeling in the reticular formation. Sparse or no anterogradely labeled fibers were seen in the mesen-

Table 2. The numbers of retrogradely labeled neurons in the SCN and the densities of anterogradely labeled varicose fibres in cholinergic, orexin, and aminergic cell groups following injections of BDA or BDA+CTB in the MPA[a]

Case	504	**481**	**472**	**473**	**482**	406	453	407*	**503**	**501**
Tracer injection										
Site[1]	MPA (LS)	MPA (LS)	MPA (LS)	MPA	MPA	MPA (BST)	MPA, PVH (Re)	BST (MPA, AH)	MPA, PVH (AH, Re)	MPA, PVH (AH, Re)
AP	−0.3	−0.3	−0.3	−0.4	−0.8	−0.92	−1.3	−1.3	−1.4	−1.4
ML	0.2	0.4	0.6	0.2	0.4	0.8	0.1	0.9	0.4	0.4
DV	7.8	8.6	8.6	8.6	8.6	7.8	7.6	8.0	8.2	8.6
Size	M	L	M/L	M/L	L	L	M	S	L	L
Tracers	BDA+CTB	BDA+CTB	BDA+CTB	BDA+CTB	BDA+CTB	BDA	BDA	BDA	BDA+CTB	BDA+CTB
Numbers of retrogradely labeled neurons[2]										
SCN shell	(0)	16	39	58	25	0	0		(4)	(2)
SCN core	(1)	10	13	16	2	0	3	0	(6)	(4)
Densities of anterograde labeling in wake-related cell groups[3]										
Cholinergic cell groups										
Medial septum–vertical diagonal band	n.a.	+	n.a.	n.a.	−/+	++/+++	−/+	+	+	+
Horizontal diagonal band	+	+/++	−/+	−/+	−/+	+	−/+	−/+	+	+
Magnocellular preoptic nucleus	−/+	−/+	−/+	−	−/+	−/+	−	−	−/+	−/+
Substantia innominata	+	++/+++	++	++	++/+++	−/+	−/+	−/+	+	−/+
Pedunculopontine tegmental nucleus	−	n.a.	−	−	n.a.	n.a.	−	n.a.	−/+	−/+
Laterodorsal tegmental nucleus	−/+	n.a.	−/+	−/+	n.a.	n.a.	−/+	n.a.	−/+	−/+
Orexin/hypocretin-containing cell group										
Orexin field, medial	+++	+++	++/+++	++/+++	+++	n.a.	−	n.a.	++/+++	++/+++
Orexin field, lateral	++	++	++	+	++	n.a.	−	n.a.	+/++	+
Aminergic cell groups										
Tuberomammillary nucleus, dorsal	++	++	++	++	++	n.a.	++	n.a.	++	++
Tuberomammillary nucleus, ventral	++	+	++	+/++	+	n.a.	+	n.a.	+	++
Ventral tegmental area	+/++	n.a.	−/+	−/+	n.a.	n.a.	−/+	n.a.	+	+
Substantia nigra, pars compacta	−/+	n.a.	−/+	−/+	n.a.	n.a.	−/+	n.a.	−/+	+
Dorsal raphe nucleus	+	n.a.	+/++	+	n.a.	n.a.	−/+	n.a.	+	++
Locus coeruleus, dendritic region	++	n.a.	+++	++/+++	n.a.	n.a.	−/+	n.a.	n.a.	++
Locus coeruleus, cell body region	+	n.a.	+	+	n.a.	n.a.	−/+	n.a.	n.a.	+/++
Other cell groups										
Mesencephalic reticular formation	−/+	n.a.	−/+	−/+	n.a.	n.a.	−	n.a.	−/+	−/+
Pontine reticular formation	−	n.a.	−/+	−	n.a.	n.a.	−	n.a.	−/+	−/+

[a] Injection sites and retrograde labeling data are adapted from Deurveilher et al. (2002). Cases with strong retrograde labeling in the SCN *and* strong anterograde labeling in a target are indicated in bold numbers in the first row, and the prominent parts of their data are shaded. CTB was used at a concentration of 0.25% in all cases except for cases 472 and 473, in which CTB was used at 0.5%. BDA was used at the concentration of 10% in all cases. The asterisk for case 407 indicates that the injection site was a "miss," i.e., centered outside of the MPA.

[1] Major and, in parentheses, minor structures involved in the injection sites are indicated. Coordinates indicate the location of the center of the core of each injection site: Anterior-posterior (AP) from bregma; mediolateral (ML) from midline; dorsoventral (DV) from skull surface (in mm). Size of injection: L, large; M, medium; S, small.

[2] The number of retrogradely labeled neurons in the SCN is based on an average of counts at three rostrocaudal levels. For the cases using injections of a BDA/CTB mixture, the results with CTB labeling are shown; when the CTB retrograde labeling could not be determined for technical reasons, the results with BDA labeling are shown in parentheses. n.a., not available; n.d., not determined.

[3] The densities of varicose fibers anterogradely labeled with BDA in cholinergic, orexin/hypocretin-containing and aminergic cell groups were based on an average over two or three levels: − no labeling; + low density; ++ moderate density; +++ dense density.

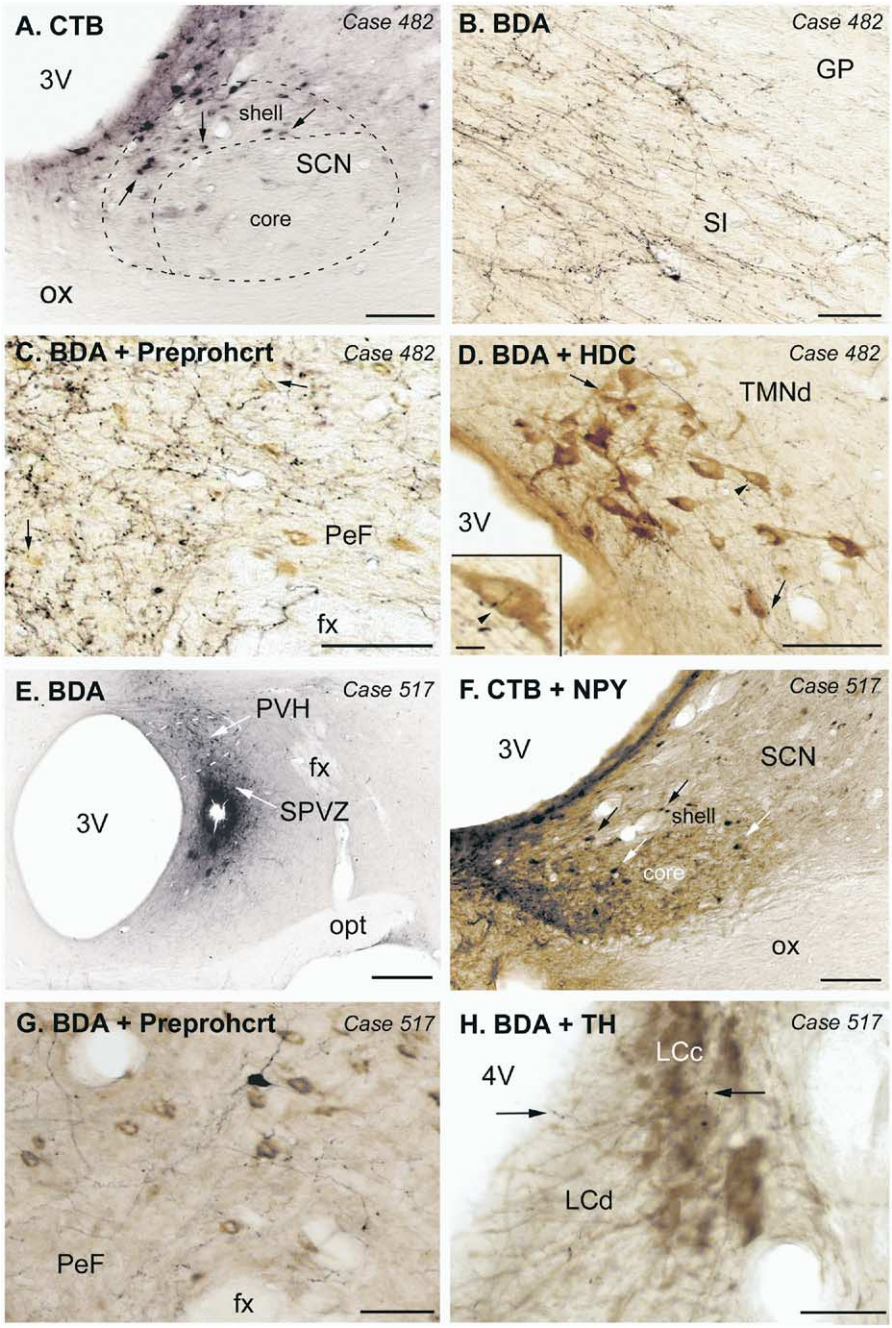

Fig. 2. Examples of retrograde labeling in the SCN and anterograde labeling in selected centers of the arousal system following BDA+CTB injection into the MPA (A–D; case 482) and the SPVZ (E–H; case 517). All images are ipsilateral to the injection site (i.e. right side of the brain). Photomicrographs of the injection site revealed for CTB and for BDA in case 482 have been shown in Deurveilher et al. (2002). (A) In the SCN, CTB-labeled neurons (arrows) are distributed mostly in the shell rather than the core region. The shell and core regions are depicted in dotted lines based on vasopressin and NPY immunoreactivity, respectively, from a separate series of sections. Several retrogradely labeled neurons are also seen in adjacent regions, particularly dorsomedial to the SCN. (B) In the basal forebrain, BDA-labeled fibers and terminals, rated as "moderate-dense" in density, are present in the substantia innominata. Most terminals appear to be of the en passant type. (C) In the perifornical area, BDA-labeled varicose axons (arrows) are mixed with preprohypocretin-ir or orexin perikarya (brown cells). (D) In the dorsal tuberomammillary nucleus, many BDA-labeled bouton-like swellings (arrows) are closely associated with HDC-ir or histaminergic neurons (brown cells). The inset shows one such HDC-ir neuron (arrowhead) along with a closely apposing BDA-labeled varicose axon at a higher magnification. (E) BDA injection site in the SPVZ. The hole at the center of the injection site is an artifact due to tissue crack. (F) In the SCN, CTB-labeled neurons are present in both the shell and core regions (examples of labeled neurons indicated by black and white arrows, respectively). Note that the SCN core contains NPY-ir fibers (brown). (G) In the perifornical area, most BDA-labeled terminals (black) do not show obvious association with orexinergic or preprohypocretin-ir perikarya (brown cells). A retrogradely labeled neuron is also present (black cell). (H) In the locus coeruleus, a few BDA-labeled fibers (arrows) are seen in the dendritic (LCd) and the core regions of the locus coeruleus (LCc; brown somata and dendrites) visualized with TH immunoreactivity. For other abbreviations, see Table 1. Scale bars=100 μm (A–D, F); 500 μm (E); 50 μm (G, H); 20 μm (inset in D).

Table 3. The numbers of retrogradely labeled neurons in the SCN and the densities of anterogradely labeled varicose fibres in cholinergic, orexin, and aminergic cell groups following injections of BDA or BDA+CTB in the SPVZ[a]

Case	402	400	**517**	471	399	**470**	**518**	485	499	**511**	498*
Tracer injection											
Site	SPVZ, RCh, PVH (MPA, AH)	PVH, SPVZ, (AH, Re, AM)	SPVZ, PVH (AH, VMH, Re, AM)	SPVZ, PVH (AH, Re)	SPVZ (PVH)	PVH, SPVZ (AH, Re, AM)	SPVZ, VMH, AH, PVH (DMH, Re)	PVH, SPVZ (AH, Re, AM)	SPVZ, AH, PVH (Re)	SPVZ, AH, PVH (DMH, Re)	AH (SPVZ)
AP	−1.6	−1.8	−1.8	−1.8	−2.12	−2.12	−2.12	−2.12	−2.12	−2.12	2.3
ML	0.4	0.2	0.3	0.6	0.1	0.2	0.4	0.6	0.8	0.8	0.8
DV	9.2	8.0	8.7	8.2	9.4	8.3	9.2	8.2	8.2	8.4	8.6
Size	L	M	M	S/L	M	M/L	L	L	M	L	S
Tracers	BDA	BDA	BDA+CTB	BDA+CTB	BDA	BDA+CTB	BDA+CTB	BDA+CTB	BDA+CTB	BDA+CTB	BDA+CTB
Numbers of retrogradely labeled neurons											
SCN shell	16	1	13	4	14	(1)	(6)	(0)	(0)	17	(0)
SCN core	22	2	10	5	9	(3)	(4)	(0)	(0)	12	(0)
Densities of anterograde labeling in wake-related cell groups											
Cholinergic cell groups											
Medial septum–– vertical diagonal band	−/+	−/+	−/+	n.a.	−/+	n.a.	+	+/++	++	+	+/++
Horizontal diagonal band	−	−/+	−/+	−	−/+	−	−/+	+/++	++	−/+	+
Magnocellular preoptic nucleus	−	−	−/+	−	−	−/+	−/+	−/+	−/+	−/+	−/+
Substantia innominata	−/+	−	−/+	−/+	−/+	−/+	−/+	−/+	−/+	−/+	−/+
Pedunculopontine tegmental nucleus	n.a.	n.a.	−	n.a.	n.a.	n.a.	−/+	+	−	−	n.a.
Laterodorsal tegmental nucleus	n.a.	n.a.	−/+	n.a.	n.a.	n.a.	−/+	+	−/+	−/+	n.a.
Orexin/hypocretin-containing cell group											
Orexin field, medial	n.a.	n.a.	++	+/++	n.a.	++	++	n.d.	++	+++	n.a.
Orexin field, lateral	n.a.	n.a.	+	+	n.a.	−/+	+	n.d.	+	++	n.a.
Aminergic cell groups											
Tuberomammillary nucleus, dorsal	n.a.	n.a.	+++	+/++	n.a.	+/++	++	++	+	++	n.a.
Tuberomammillary nucleus, ventral	n.a.	n.a.	++	−/+	n.a.	n.d.	−/+	+/++	+	+	
Ventral tegmental area	n.a.	n.a.	−/+	n.a.	n.a.	n.a.	−/+	+	−	−/+	n.a.
Substantia nigra, pars compacta	n.a.	n.a.	−/+	n.a.	n.a.	n.a.	+	+	−/+	−/+	n.a.
Dorsal raphe nucleus	n.a.	n.a.	+	n.a.	n.a.	n.a.	−/+	+	+	−/+	n.a.
Locus coeruleus, dendritic region	n.a.	n.a.	+/++	n.a.	n.a.	n.a.	+/++	+	−/+	−/+	n.a.
Locus coeruleus, cell body region	n.a.	n.a.	+	n.a.	n.a.	n.a.	−/+	−	−	−	n.a.
Other cell groups											
Mesencephalic reticular formation	n.a.	n.a.	−/+	n.a.	n.a.	n.a.	−/+	−/+	−/+	−/+	n.a.
Pontine reticular formation	n.a.	n.a.	−	n.a.	n.a.	n.a.	−/+	−/+	−	−/+	n.a.

[a] The injection sites and retrograde labeling data are adapted from Deurveilher et al. (2002). Cases with strong retrograde labeling in the SCN *and* strong anterograde labeling in a target are indicated in bold case numbers in the first row, and the prominent parts of their data are shaded. The asterisk for case 498 indicates that the injection was a "miss" and was centered outside of the SPVZ. CTB was used at a concentration of 0.25% in all cases except for cases 470 and 471, in which CTB was used at 0.5%. Each number of retrogradely labeled neurons in the SCN represents an average of counts from three levels except for cases 400, 499 and 518, in which an average of counts from two levels was used. See footnotes to Table 2 for further details.

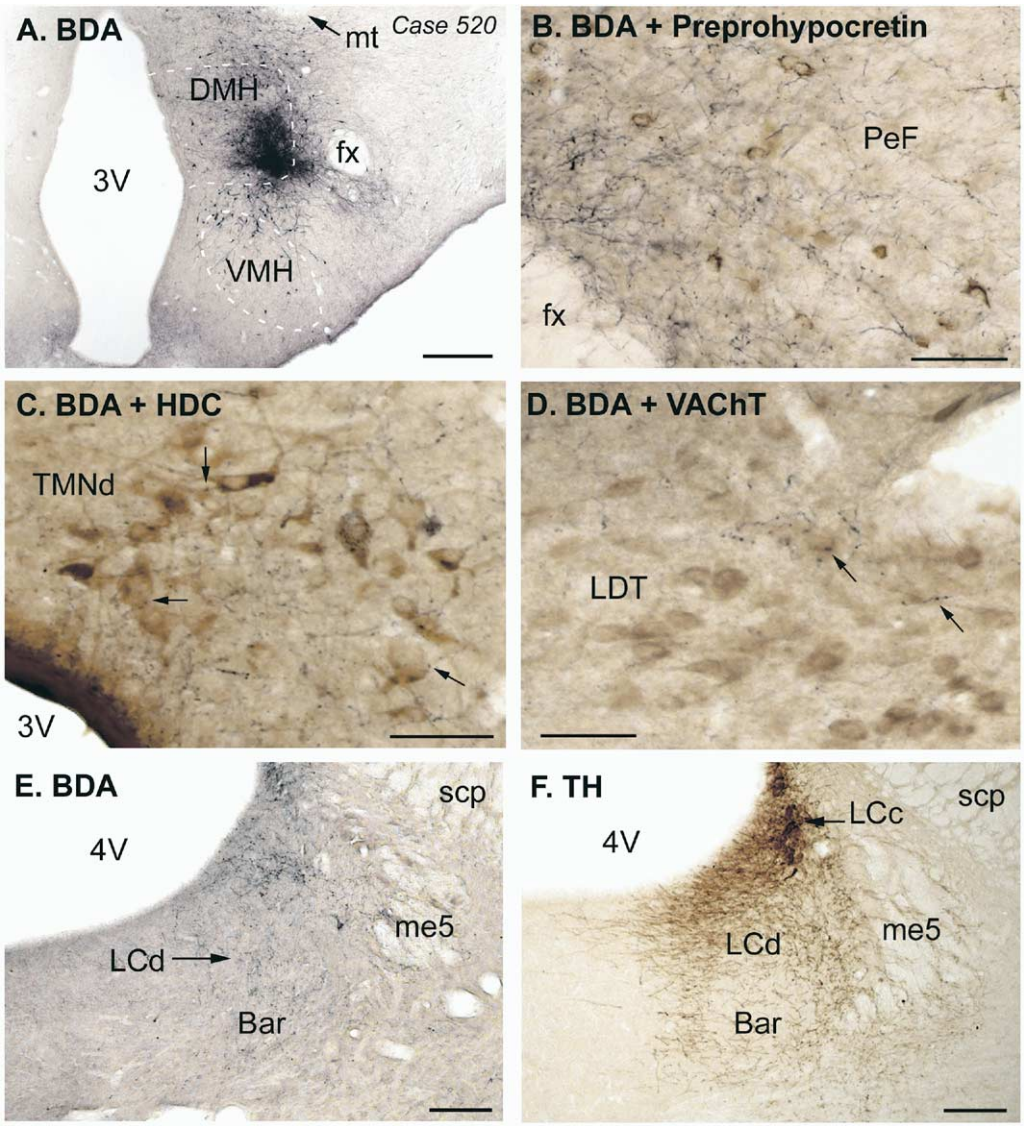

Fig. 3. Photomicrographs showing the anterograde labeling in selected centers of the arousal system following BDA+CTB injection into the caudal DMH (case 520). (A) The relatively small injection site revealed for BDA is located in the ventrolateral aspect of the caudal DMH. (B) In the lateral perifornical area, BDA-labeled fibers (black) are present among preprohypocretin-ir (orexin) neurons (brown). (C) In the dorsal tuberomammillary nucleus, some BDA bouton-like swellings (arrows) are closely associated with HDC-ir (histaminergic) cell bodies and dendrites (brown). (D) In the laterodorsal tegmental nucleus, close associations are seen between BDA-labeled terminals (arrows) and VAChT-ir (cholinergic) cell bodies (brown cells). (E) The dendritic region of the locus coeruleus, which also overlaps with Barrington's nucleus, contains moderately abundant BDA-labeled varicose fibers. (F) This section at the same level as in E was stained for TH to visualize noradrenergic cell bodies and dendrites. For abbreviations, see Table 1. Scale bars=500 μm (A), 100 μm (B, E, F), 50 μm (C, D).

cephalic and pontine reticular fields in any of the MPA cases (Table 2).

In summary, the results based on both CTB and BDA labeling indicate that the MPA receives strong projections from the SCN and, in turn, provides strong projections to the orexin field, the tuberomammillary nucleus, and the locus coeruleus dendritic region (which also overlaps with Barrington's nucleus). The projections to the substantia innominata originate mostly from the rostral MPA. These results indicate that the MPA is a strong candidate for a relay in respective indirect pathways from the SCN.

The SPVZ

The retrograde labeling with either CTB or BDA indicated that the SCN projections to the SPVZ region arose equally from the shell and the core (Table 3). Numerous retrogradely labeled neurons were also present in the ventral part of the lateral septum, bed nucleus of the stria terminalis, anteroventral periventricular and ventromedial hypothalamic nuclei (Deurveilher et al., 2002). Anterograde BDA labeling was analyzed in five cases for both forebrain and brainstem, and in six cases for forebrain only (Table 3). Of these 11 cases, seven with the largest numbers of

retrogradely labeled neurons in the SCN are described in detail. These seven injections were centered medially (ML 0.1–0.4) or laterally (ML 0.6–0.8) within the SPVZ. An example of a medium-sized injection in the SPVZ, and retrograde labeling in the SCN after this injection are shown in Fig. 2E and F, respectively (case 517).

Anterograde labeling in the cholinergic cell regions. All seven SPVZ injections that yielded strong retrograde labeling in the SCN produced only sparse to low, or no anterograde labeling in any of the four basal forebrain cholinergic cell regions examined (Table 3). Five of these seven injections were located medially in the SPVZ (399, 400, 402, 470 and 517), one was centered in the lateral SPVZ (511), and the other involved both the medial and lateral SPVZ (518). Three injections that resulted in only minor retrogradely labeled neurons in the SCN (471, 485 and 499) were located in the lateral SPVZ, and yielded denser labeling in the MS-VDB and HDB (mostly low-moderate to moderate) than in more caudal basal forebrain regions, with the exception of case 471 which provided sparse or no labeling in any basal forebrain region examined. A small injection that missed the SPVZ and was centered laterally in the anterior hypothalamic area but with minor diffusion into the SPVZ resulted in stronger anterograde labeling in the rostral than the caudal basal forebrain regions (498). In the brainstem, all SPVZ injections produced sparse or no anterograde labeling in the pedunculopontine and laterodorsal tegmental nuclei.

Functional differences have been reported between the ventral and the dorsal SPVZ in their roles in circadian rhythms of sleep, locomotion and temperature (Lu et al., 2001), and therefore we examined the injection sites using this scheme in an attempt to identify possible differences in the pattern of anterograde labeling. Of the seven injections in the SPVZ that yielded strong retrograde labeling in the SCN, only one injection (case 402) was located in the ventral SPVZ, whereas the other six injections were in the dorsal SPVZ. The density of anterograde labeling within the basal forebrain cholinergic cell groups in the ventral SPVZ case (402) did not differ from that in the dorsal SPVZ cases. Unfortunately, the anterograde labeling in the other forebrain regions and the brainstem in case 402 could not be analyzed for a technical reason, which precluded further comparisons.

Anterograde labeling in the orexin cell region. The injections in the SPVZ resulting in strong retrograde labeling in the SCN produced denser anterograde labeling in the medial (moderate to dense) than in the lateral (sparse to moderate) region of the orexin field (470, 511, 517 and 518; Table 3). Varicose fibers labeled from the SPVZ were interspersed with orexin-ir cell bodies and dendrites, particularly with the more lateral SPVZ injections (517, Fig. 2G). Similarly, injections with little or no retrograde labeling in the SCN showed denser labeling in the medial than in the lateral part of the orexin field (471 and 499).

It should be noted that injections in the SPVZ resulted in moderate to dense anterograde labeling in the DMH. Given that the medial part of the box used to assess BDA labeling in the orexin field partly overlapped with the lateral region of the DMH, the projections of the SPVZ to the medial orexin field may be considered to be part of the SPVZ projections to the DMH reported by Watts et al. (1987) and Chou et al. (2003).

Anterograde labeling in the aminergic cell regions. The SPVZ injections that resulted in strong retrograde labeling in the SCN produced moderate to dense anterograde labeling in the dorsal tuberomammillary nucleus, which was the densest of all aminergic cell groups examined. Many anterogradely labeled terminals were found in the vicinity of HDC-ir cell bodies and dendrites (511, 517 and 518; Table 3). Only sparse to moderate labeling was seen in the ventral tuberomammillary nucleus, and sparse to low anterograde labeling in the ventral tegmental area, substantia nigra pars compacta, and dorsal raphe nucleus. The dendritic region of the locus coeruleus showed sparse to low-moderate labeling, while the core region showed only low or no labeling (Fig. 2H). Similarly, even the SPVZ injections resulting in little or no retrograde labeling in the SCN produced generally denser anterograde labeling in the tuberomammillary nucleus than in the other brainstem nuclei examined (485 and 499).

Anterograde labeling in the reticular formation. All SPVZ injections produced sparse or no anterograde labeling in the mesencephalic and pontine reticular formation (Table 3).

In summary, the SPVZ receives strong projections from the SCN and, in turn, sends strong projections to both the orexin field and tuberomammillary nucleus, indicating that the SPVZ is a strong candidate relay nucleus in these indirect pathways from the SCN. The SPVZ does not appear to be positioned to relay the SCN projections further caudally to the brainstem.

The DMH

The retrograde labeling data indicated that the SCN projections to the rostral DMH arose equally from the shell and core, whereas those to the caudal DMH originated predominantly from the shell (Table 4). In addition to SCN neurons, numerous retrogradely labeled neurons were found in the lateral septum, bed nucleus of the stria terminalis, anteroventral periventricular nuclei, anterior hypothalamic nucleus, and dorsal tuberomammillary nucleus (Deurveilher et al., 2002). Anterograde BDA labeling was analyzed in five cases for both forebrain and brainstem, and in three cases for forebrain only (Table 4). Of these eight cases, five with the highest numbers of retrogradely labeled neurons in the SCN are described below in detail, whereas the other three producing less retrograde labeling provided supplementary data. An example of a small injection site in the DMH is shown in Fig. 3A (case 520).

Anterograde labeling in the cholinergic cell regions. A small injection that was largely confined to the caudal DMH (520) and yielded strong retrograde labeling in the SCN resulted in sparse to low anterograde labeling in the

Table 4. The numbers of retrogradely labeled neurons in the SCN and the densities of anterogradely labeled varicose fibers in cholinergic, orexin, and aminergic cell groups following injections of BDA or BDA+CTB in the DMH[a]

Case	415	483	**490**	**512**	**409**	**520**	**515**	514*
Tracer injection								
Site	DMH, DA (AH, VMH, Re, CM)	DMH, DA (VMH, AH, Re)	DMH, VMH (DA, AH)	DMH (DA, AH, VMH, Re)	DMH (DA, PH, Re)	DMH	DMH (PH, TMNd)	PeF (DMH)
AP	−2.56	−2.8	−3.14	−3.14	−3.3	−3.3	−3.3	−3.3
ML	0.6	0.6	0.6	0.8	0.4	0.8	0.8	1.1
DV	8.6	8.6	9.0	8.8	8.8	9.2	9.2	8.8
Size	L	L	L	L	M	S	L	S
Tracers	BDA	BDA+CTB	BDA+CTB	BDA+CTB	BDA	BDA+CTB	BDA+CTB	BDA+CTB
Numbers of retrogradely labeled neurons								
SCN shell	0	2	12	8	4	5	27	1
SCN core	0	2	13	11	3	2	13	0
Densities of anterograde labeling in wake-related groups								
Cholinergic cell groups								
Medial septum–vertical diagonal band	−/+	n.a.	−/+	−/+	++/+++	+	+++	+
Horizontal diagonal band	−/+	−/+	−/+	−/+	+/++	−/+	+++	+
Magnocellular preoptic nucleus	−/+	−/+	−/+	−/+	−/+	−/+	+/++	−/+
Substantia innominata	−/+	−/+	−/+	−/+	−/+	−/+	+++	++
Pedunculopontine tegmental nucleus	n.a.	n.a.	−	−/+	n.a.	−/+	+/++	−/+
Laterodorsal tegmental nucleus	n.a.	n.a.	−/+	+/++	n.a.	+/++	++	+/++
Orexin/hypocretin-containing cell group								
Orexin field, medial	n.a.	n.d.	n.d.	n.d.	n.d.	n.d.	n.d.	n.d.
Orexin field, lateral	n.a.	+	n.d.	++/+++	n.d.	++/+++	+++	n.d.
Aminergic cell groups								
Tuberomammillary nucleus, dorsal	n.a.	++	++/+++	++/+++	+++	+++	n.d.	+/++
Tuberomammillary nucleus, ventral	n.a.	−/+	+/++	−/+	n.d.	++	n.d.	+/++
Ventral tegmental area	n.a.	n.a.	+	−/+	n.a.	++	+++	+/++
Substantia nigra, pars compacta	n.a.	n.a.	+	−/+	n.a.	+	++	+
Dorsal raphe nucleus	n.a.	n.a.	+/++	++	n.a.	++	+++	++
Locus coeruleus, dendritic region	n.a.	n.a.	−/+	−/+	n.a.	++/+++	+++	+++
Locus coeruleus, cell body region	n.a.	n.a.	−	−/+	n.a.	+	++	−/+
Other cell groups								
Mesencephalic reticular formation	n.a.	n.a.	+/++	+	n.a.	−/+	++	+/++
Pontine reticular formation	n.a.	n.a.	−	−/+	n.a.	−/+	++	+

[a] The injection sites and retrograde labeling data are adapted from Deurveilher et al. (2002). Cases with strong retrograde labeling in the SCN *and* strong anterograde labeling in a target are indicated in bold case numbers in the first row, and the prominent parts of their data are shaded. The asterisk for case 514 indicates that the injection was a "miss" and centered outside of the DMH. See footnotes to Table 2 for further details.

cholinergic cell regions of the basal forebrain (Table 4). A medium-sized injection at the same rostrocaudal level that diffused into the PH (409) revealed stronger (moderate-dense) labeling in the MS-VDB than in the HDB (low-moderate), magnocellular preoptic nucleus or substantia innominata (sparse). A large injection at the same rostrocaudal level of the DMH but extending into the PH (515) produced dense labeling in the MS-VDB, HDB and substantia innominata, but only low-moderate labeling in the magnocellular preoptic nucleus. In contrast, two large injections centered at the rostral DMH and extending rostrally into the posterior part of the anterior hypothalamic nucleus, and ventrally into the dorsal division of the ventromedial hypothalamic nucleus (490 and 512) provided sparse anterograde labeling in all basal forebrain cholinergic regions examined.

In the brainstem, caudal DMH injections (515 and 520) produced low-moderate to moderate labeling in the laterodorsal tegmental nucleus, whereas sparse to low-moderate labeling in the pedunculopontine tegmental nucleus (Table 4). BDA-stained varicose axons were seen near VAChT-ir cell bodies and dendrites in the laterodorsal tegmental nucleus (Fig. 3D). Labeling was lighter following rostral DMH injections (490 and 512).

Two injections centered at the rostral DMH (415 and 483) yielded little or no retrograde labeling in the SCN, and produced only sparse labeling in all the basal forebrain cholinergic cell regions, consistent with the above results. A small injection (514) that fell in the perifornical area lateral to the DMH produced denser anterograde labeling in the substantia innominata and laterodorsal tegmental nucleus than in the other areas examined.

Anterograde labeling in the orexin cell region The lateral region of the orexin field contained moderate-dense to dense anterograde labeling from the DMH (512, 515 and 520; Table 4). Varicose fibers labeled following DMH injections were found near orexin-ir cell bodies and proximal dendrites (Fig. 3B). The anterograde labeling in the medial part of the orexin field after DMH injections could not be analyzed because of the proximity of the injection sites or the diffusion of the tracer.

Anterograde labeling in the aminergic cell regions. Two caudal DMH injections (409 and 520) with strong retrograde labeling in the SCN produced moderate to dense labeling in both the dorsal and ventral regions of the tuberomammillary nucleus (Table 4). BDA-stained varicose axons were seen near HDC-ir cell bodies and dendrites (Fig. 3C). Labeling could not be analyzed in case 515, a third caudal DMH case, because of tracer diffusion into the dorsal tuberomammillary nucleus. In cases 515 and 520, labeling in the ventral tegmental area and substantia nigra was moderate to dense, and low to moderate, respectively. Terminal-laden axons were intermixed with TH-ir somata and dendrites. Moderate to dense labeling was found in the dorsal raphe nucleus, where BDA-labeled varicose fibers were seen intermingled with serotonin-ir cell bodies and dendrites. The dendritic region of the locus coeruleus showed moderate-dense to dense labeling, while the cell body region showed low to moderate labeling (Fig. 3E, F). Many BDA-labeled varicose fibers were intermingled with TH-ir dendrites, while few BDA-stained varicosities were seen between TH-positive cell bodies in the nuclear core.

As was the case for caudal DMH injections, two rostral DMH injections with strong retrograde labeling in the SCN (490 and 512) produced denser anterograde labeling in the dorsal (moderate-dense) than in the ventral tuberomammillary nucleus (sparse to low-moderate; Table 4). The density in the dorsal raphe nucleus was low-moderate to moderate. In contrast to caudal DMH injections, however, only sparse to low or no labeling was observed in the other aminergic areas analyzed.

An injection (514) located in the perifornical area produced denser anterograde labeling in the dorsal raphe nucleus and the dendritic region of the locus coeruleus than in the other target areas examined.

Anterograde labeling in the reticular formation. Only in the case of a large injection in the caudal DMH was moderate labeling seen in the mesencephalic and pontine reticular fields (515). Lighter labeling was seen after a small injection at the same level of the DMH (520), injections in the rostral DMH (490 and 512), or an injection in the perifornical area (514).

In summary, the DMH receives dense projections from the SCN and, in turn, sends dense projections to the orexin field and tuberomammillary nucleus. In addition, the caudal DMH projects to brainstem regions including the ventral tegmental area, dorsal raphe nucleus, laterodorsal tegmental nucleus, and locus coeruleus dendritic region. These results indicate that the DMH is a strong relay candidate.

The PH

The SCN projections to the PH are limited; only in one case (519), in which injection was centered in the rostral PH but spread into the caudal DMH, dense retrograde labeling was seen in the SCN, prominently in the shell (Table 5). In this case, as was found after caudal DMH injections, anterograde labeling was the densest (moderate to dense) in the orexin field, dorsal raphe nucleus and locus coeruleus dendritic region (Table 5). Numerous BDA-labeled varicosities were mixed with immunolabeled cell bodies and dendrites in all these areas. Only sparse to low-moderate labeling was seen in the other aminergic and cholinergic cell groups, and in the mesencephalic and pontine reticular fields.

The four injections centered at the rostral PH with little (411 and 513) or no diffusion into the DMH (491 and 523) resulted in more limited retrograde labeling in the SCN than when the injection spread to the DMH (case 519; Table 5). Anterograde labeling in the cholinergic and orexin cell groups, mesencephalic and pontine reticular fields, was comparable to case 519, except that the density in the rostral cholinergic cell groups was higher in case 513, and the labeling in the orexin field in case 491 was less than in case 519. As in case 519, the anterograde

Table 5. The numbers of retrogradely labeled neurons in the SCN and the densities of anterogradely labeled varicose fibres in cholinergic, orexin, and aminergic cell groups following injections of BDA or BDA+CTB in the PH[a]

Case	**519**	411	513	522	521*	491	523
Tracer injection							
Site	PH (DMH, TMNd)	PH (DMH, DA)	PH (DMH, Re)	PeF, PH (DMH)	TMNd (PH)	PH (SP, CM)	PH (TMNd)
AP	−3.6	−3.6	−3.6	−3.6	−3.8	−3.8	−3.8
ML	0.2	0.5	0.6	0.8	0.2	0.8	0.4
DV	8.8	8.4	8.6	8.6	9.1	8.8	8.8
Size	M	M	M	M	S	L	M
Tracers	BDA+CTB	BDA	BDA+CTB	BDA+CTB	BDA+CTB	BDA+CTB	BDA+CTB
Numbers of retrogradely labeled neurons in SCN							
SCN shell	44	0	2	(1)	2	1	2
SCN core	28	0	0	(0)	2	3	0
Densities of anterograde labeling in wake-related cell groups							
Cholinergic cell groups							
Medial septum–vertical diagonal band	+	++	++	+/++	−/+	n.a.	+/++
Horizontal diagonal band	+	−/+	+++	+	+	+	+
Magnocellular preoptic nucleus	−/+	−/+	−/+	−/+	−/+	−/+	−
Substantia innominata	+	−/+	+	++/+++	+	+	+/++
Pedunculopontine	−/+	n.a.	++	+/++	−/+	n.a.	−/+
Laterodorsal tegmental nucleus	+/++	n.a.	++/+++	++	++	n.a.	−/+
Orexin/hypocretin-containing cell group							
Orexin field, medial	+++	+++	+++	n.d.	+++	+	+++
Orexin field, lateral	++	++/+++	+++	n.d.	++	+	++
Aminergic cell groups							
Tuberomammillary nucleus, dorsal	n.d.	n.a.	++	+/++	n.d.	+	n.d.
Tuberomammillary nucleus, ventral	n.d.	n.a.	++	++	n.d.	−	n.d.
Ventral tegmental area	+/++	n.a.	+/++	++	−/+	n.a.	+
Substantia nigra, pars compacta	−/+	n.a.	+/++	+/++	−/+	n.a.	−/+
Dorsal raphe nucleus	++	n.a.	+++	++	+/++	n.a.	+
Locus coeruleus, dendritic region	++	n.a.	+++	++	++	n.a.	++
Locus coeruleus, cell body region	+	n.a.	+/++	+	+	n.a.	−/+
Other cell groups							
Mesencephalic reticular formation	−/+	n.a.	+	+/++	−/+	n.a.	−/+
Pontine reticular formation	−/+	n.a.	+/++	+	−/+	n.a.	+

[a] The injection sites and retrograde labeling data are adapted from Deurveilher et al. (2002). A case with strong retrograde labeling in the SCN *and* strong anterograde labeling in a target is indicated in bold case number in the first row, and the prominent parts of its data are shaded. The asterisk for case 521 indicates that the injection was a "miss", i.e., centered outside of the PH. See footnotes to Table 2 for further details.

labeling in the dorsal raphe nucleus and the locus coeruleus dendritic region was denser than in the other aminergic areas examined (513 and 523).

One injection centered in the perifornical area (522) with significant diffusion into the PH resulted in little retrograde labeling in the SCN; the density of anterograde labeling appeared similar to that seen in case 519 in all regions examined. A small injection centered at the dorsal tuberomammillary nucleus (521) with minor diffusion into the PH produced little retrograde labeling in the SCN; the density of anterograde labeling was roughly comparable to that seen in case 519 in all cell groups examined.

In summary, the retrograde labeling results indicate that the PH is unlikely to be a relay nucleus. In fact, only the single case (519) in which the injection diffused into the caudal DMH, but not the cases with little or no diffusion in the DMH, showed dense retrograde labeling in the SCN. Nonetheless, the efferent projections of the caudal DMH and rostral PH might overlap, because the anterograde labeling results of case 519 were for the most part similar to those seen after the caudal DMH injections.

DISCUSSION

The present results using a combination of anterograde and retrograde tract-tracing techniques show that the MPA, SPVZ and DMH are potential relay nuclei for indirect SCN projections to the major arousal/wake-regulatory neuronal groups in the brain. Specifically, all these preoptic and hypothalamic nuclei receive strong afferent projections from the SCN, either from the shell or from both the shell and core, as reported previously (Watts and Swanson, 1987; Leak and Moore, 2001; Deurveilher et al., 2002). These nuclei, in turn, send projections of variable magnitudes to the cholinergic, orexin and aminergic cell groups involved in arousal, as summarized in Fig. 4. The MPA projections mainly innervate the substantia innominata, orexin cell region and dorsal tuberomammillary nucleus in the forebrain, and the locus coeruleus dendritic region (which also overlaps with Barrington's nucleus) in the brainstem. The SPVZ projections are largely confined to the hypothalamus, with the heaviest to the medial orexin field and the dorsal tuberomammillary nucleus. The DMH

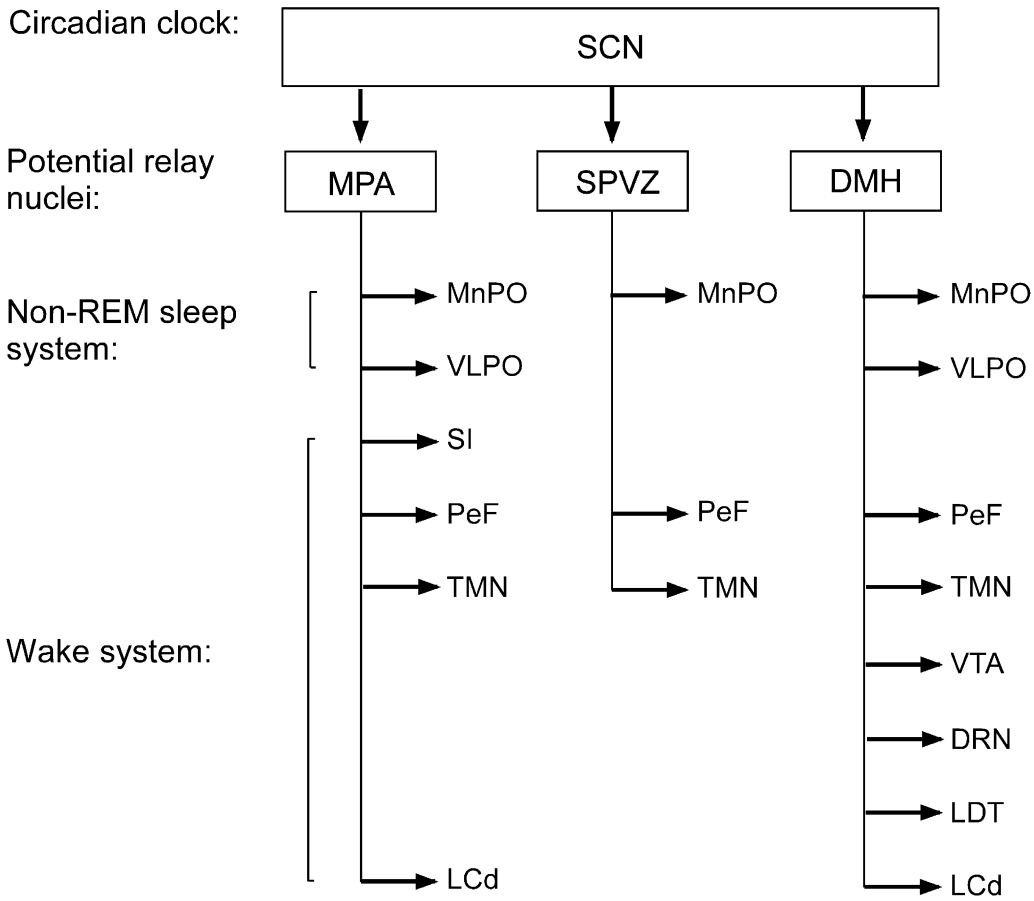

Fig. 4. A schematic illustrating the organization of potential indirect SCN neuronal output pathways to major sleep- and arousal-regulatory neuronal groups. Candidate relay nuclei in the indirect pathways are the MPA, SPVZ, and DMH. Major efferent target regions within the wake system (present study; some of these target regions are also involved in REM sleep mechanisms) and the non-REM sleep system [VLPO from Deurveilher et al. (2002) and MnPO from Deurveilher and Semba (2003)] are based on the representative examples (case 472 for MPA; case 517 for SPVZ; and case 520 for DMH) analyzed in these studies, and are arranged from rostral (top) to caudal (bottom). Indirect pathways involving more than two synapses are not included. Note the differential distributions of the efferents from the three possible intermediary nuclei. See Table 1 for abbreviations.

projections are the most extensive of all, innervating the orexin field, tuberomammillary nucleus, ventral tegmental area, dorsal raphe nucleus, laterodorsal tegmental nucleus, and locus coeruleus dendritic region. These potential indirect pathways from the SCN to different centers of the arousal system are likely to provide an anatomical substrate for the circadian control of sleep–wake states, as well as other physiological functions.

Technical considerations

We as well as others have discussed technical issues associated with the dual tract-tracing technique using co-injections of anterograde and retrograde tracers that was used in the present study (Coolen and Wood, 1998; Coolen et al., 1999; Deurveilher et al., 2002). The main limitation of this technique is that it does not allow direct examination of the relationship between input fibers and output neurons within the injection site, either at the light or electron microscopic levels. As discussed previously (Deurveilher et al., 2002), this is particularly a concern for large injections, because the afferents could be segregated from projection neurons within the same injection site. Nonetheless, there are two advantages to this technique that should not be overlooked. First, this technique is relatively simple, and is less labor-intensive and time-consuming than performing separate injections of anterograde and retrograde tracers and examining overlap between the two labels (Vrang et al., 1997; Gaus and Saper, 2000; Peng and Bentivoglio, 2004). Second, the co-injection technique allows concurrent examination of multiple targets of indirect projections. This is a considerable practical advantage, particularly if the goal is to obtain a broad picture that can be used to guide more detailed studies.

Anatomical considerations

The MPA sent its heaviest projections to the substantia innominata, orexin cell field, dorsal tuberomammillary nucleus, and locus coeruleus dendritic region. These results are generally consistent with previous studies (Chiba and Murata, 1985; Fahrbach et al., 1986; Grove, 1988; Simerly and Swanson, 1988; Ericson et al., 1991; Rizvi et al., 1994; Luppi et al., 1995; Peyron et al., 1998; Steininger et al., 2001). The DMH projected prominently to the orexin field, dorsal tuberomammillary nucleus, ventral tegmental area, dorsal raphe nucleus, laterodorsal tegmental nucleus, and locus coeruleus dendritic region. These results also generally agree with previous studies (Kalen et al., 1985; ter Horst and Luiten, 1986; Ericson et al., 1991; Semba and Fibiger, 1992; Luppi et al., 1995; Thompson et al., 1996; Peyron et al., 1998; Aston-Jones et al., 2001; Chou et al., 2003). In contrast to the MPA and DMH, the SPVZ projections were much more restricted and virtually confined to the hypothalamus, with the densest (yet moderate) projections to the dorsal tuberomammillary nucleus and the medial aspect of the orexin cell group. These limited efferent connections of the SPVZ are consistent with the previous results of an anterograde tracing study by Watts et al. (1987). We also confirmed a projection from the SPVZ to the DMH (Watts et al., 1987; Chou et al., 2003). Thus, the present findings, in conjunction with previous studies, indicate that the MPA, SPVZ and DMH, which all receive strong projections from the SCN, co-innervate several key wake-promoting cell groups, while also having distinct innervation to the other key areas within the arousal system.

For each wake-promoting cell region, possible indirect pathways from the SCN may be summarized as follows (Fig. 4): (1) the orexin cell field and tuberomammillary nucleus may receive indirect input from the SCN via the MPA, SPVZ and DMH; (2) the dendritic field of the locus coeruleus may receive indirect input from the SCN through the MPA and DMH; (3) the substantia innominata may receive an indirect SCN input via the MPA; and (4) the ventral tegmental area, dorsal raphe nucleus and laterodorsal tegmental nucleus may receive an indirect input from the SCN via the DMH. Thus, the MPA, and in particular the DMH are well positioned to convey SCN signals to both the forebrain and brainstem regions involved in wake state control. The SPVZ's ability to "broadcast," on the other hand, appears to be more limited at least on a disynaptic basis. However, in light of the projections from the SPVZ to the DMH, the DMH could act to expand the sphere of influence for the SPVZ through its projections to many brain regions that are not directly innervated by the SPVZ.

Functional evidence that wake-regulatory neuronal groups targeted by the possible indirect SCN output pathways display circadian rhythmicity

If the anatomically suggested indirect pathways are indeed functional and play a role in circadian rhythms of sleep–wake states, the neuronal activity of the target wake-promoting nuclei should show rhythmicity under constant darkness conditions, and damage to the target nuclei could disrupt circadian sleep rhythms. There is some evidence to support these predictions.

The daily rhythms of c-Fos expression in orexin neurons (Estabrooke et al., 2001; Martinez et al., 2002) and orexin levels (Taheri et al., 2000; Yoshida et al., 2001; Zeitzer et al., 2003) persisted in constant darkness (Estabrooke et al., 2001; Zhang et al., 2004), and the orexin level rhythms were abolished by SCN lesions (Zhang et al., 2004), suggesting that these rhythms are not simply driven by photic stimuli but are regulated by the endogenous circadian pacemaker. Furthermore, orexin B-saporin lesions significantly attenuated diurnal rhythms of all three behavioral states (Gerashchenko et al., 2001), whereas genetic ablation of orexin neurons attenuated diurnal REM sleep rhythms (Hara et al., 2001). These data suggest that orexin neurons may be responsible for at least some of the circadian rhythms of sleep–waking, especially of REM sleep.

Similar to orexin neurons, c-Fos expression of histaminergic neurons (Ko et al., 2003) and histamine levels (Mochizuki et al., 1992; Prast et al., 1992; Yamatodani et al., 1996) increased in the dark period in nocturnal rodents, and the rhythms of histamine levels persisted in constant

darkness (Yamatodani et al., 1996). Deletion of the HDC gene had virtually no effects on sleep–wake rhythms under light–dark (LD) conditions (Parmentier et al., 2002; Abe et al., 2004); however, it lengthened locomotor activity periods under constant darkness and dampened extra-SCN clock gene expression rhythms, suggesting a role of histamine in providing feedback to clock mechanisms, or its involvement in the output pathway (Abe et al., 2004).

Noradrenergic neurons in the locus coeruleus were more active during the dark, than the light, period in nocturnal rodents (Aston-Jones et al., 2001). These rhythms persisted in constant darkness under anesthesia, indicating that they are directly regulated by signals from the circadian clock rather than simply reflecting changes in arousal levels. DMH lesions eliminated these circadian rhythms, confirming a functional, indirect SCN-locus coeruleus pathway via the DMH (Aston-Jones et al., 2001; see also Legoratti-Sanchez et al., 1989). However, preliminary data indicated that locus coeruleus lesions did not affect circadian sleep rhythms under constant darkness (Gonzales et al., 2002), suggesting that despite its circadian neuronal activity, the locus coeruleus is not necessary for, but might participate in, circadian sleep–wake rhythms.

Similar evidence exists for the serotonergic raphe neurons and basal forebrain cholinergic neurons. Serotonin levels in specific brain areas showed daily rhythms which persisted under constant darkness, suggesting that these rhythms are controlled by the endogenous circadian clock (Semba et al., 1984; Cagampang et al., 1993). However, lesions of the dorsal raphe nucleus did not affect circadian rhythms of sleep (Mouret and Coindet, 1980). Similarly, the daily rhythm of acetylcholine levels in the frontal cortex, to which the substantia innominata projects (Wainer and Mesulam, 1990), persisted under constant darkness (Kametani and Kawamura, 1991). Immunotoxic lesions of cholinergic basal forebrain neurons, however, did not affect diurnal rhythms of sleep (Kapas et al., 1996).

Unlike the above transmitter systems, dopamine levels in brain areas innervated by the ventral tegmental area did not show diurnal variations (Paulson and Robinson, 1994; Feenstra et al., 2000). Interestingly, however, 6-hydroxydopamine lesions of ventral tegmental dopaminergic neurons slightly affected sleep–waking and activity rhythms under LD conditions (Sakata et al., 2002), and lengthened the periods of activity in blinded rats (Isobe and Nishino, 2001). Thus, the ventral tegmental dopaminergic system appears to be involved in, but not critical for, the expression of circadian rhythmicity of sleep–waking.

In conclusion, the previous studies indicate that all the transmitter-specific systems implicated in wake control, with the possible exception of the ventral tegmental dopaminergic system, show diurnal rhythms in their activity. For most regions, this rhythmicity persists under constant darkness, suggesting that these wake-promoting systems receive endogenous circadian signals from the SCN, possibly through the indirect pathways suggested by the present study. Lesion studies indicate, however, that their roles in circadian sleep–wake rhythms are not critical, although some of the wake-promoting transmitter systems, such as orexin and histamine systems, appear to play a role in the expression of circadian sleep–waking rhythms by providing feedback to clock mechanisms in the SCN, or by participating in its output pathways.

Functional evidence that the possible relay nuclei mediate the circadian signal to the sleep/wake-regulatory neuronal groups: are there segregated pathways?

The current proposal that the MPA, SPVZ and DMH relay the circadian signal to both sleep- and wake-regulatory neuronal groups (present study; Deurveilher et al., 2002; Deurveilher and Semba, 2003) requires that neurons in these potential relay nuclei be under the circadian control and therefore show circadian rhythms. However, conclusive evidence for this requirement is still lacking. For example, all of these three nuclei showed diurnal rhythms of c-Fos expression under LD conditions (Lee et al., 1998; Nunez et al., 1999; Peterfi et al., 2004). However, the persistence, in constant darkness, of the c-Fos or neuronal activity rhythms remains to be determined for the MPA and DMH, and the evidence for the SPVZ is inconclusive. Specifically, c-Fos rhythms in the ventral SPVZ were abolished in constant darkness in nocturnal (but not diurnal) rats, suggesting that they may be dependent on photic input at least in this species (Schwartz et al., 2004). Yet, daily rhythms of neural activity in the region surrounding the SCN (which presumably included the ventral SPVZ) persisted in constant darkness in nocturnal rats (Inouye and Kawamura, 1979), suggesting that the neural activity in this area may show circadian rhythms in the absence of c-Fos rhythms. The reason for this discrepancy is unclear.

Despite the incomplete evidence for the presence of circadian rhythms in the proposed relay nuclei, the importance of the SPVZ and DMH as circadian relays has been demonstrated by lesion studies. Excitotoxic lesions of ventral and dorsal SPVZ reduced circadian rhythms of sleep, locomotor, and temperature rhythms, respectively (Lu et al., 2001), and DMH lesions disrupted circadian rhythms of wakefulness, locomotor activity, as well as feeding and serum corticosteroid levels (Chou et al., 2003). Excitotoxic or radiofrequency lesions of the MPA also reduced diurnal rhythms of sleep (Asala et al., 1990; Lu et al., 2000). However, the animals were not tested under constant darkness in these studies, and this remains as a subject for future research.

As sleep and wake are opposing processes, it is possible that different relay neurons are responsible for conveying the circadian signal to sleep vs. wake centers. The MPA has long been known to be involved in the promotion of sleep, possibly by exerting an inhibitory influence upon the arousal system (e.g. Szymusiak and McGinty, 1989; Asala et al., 1990; Behbehani and Da Costa Gomez, 1996; Lu et al., 2000; Methippara et al., 2003). In contrast, evidence based on lesions and stimulation suggests that the DMH exerts an excitatory influence upon the arousal system (Zaretskaia et al., 2002; Chou et al., 2003). We found that each of the proposed relay nuclei projected to both sleep- and wake-promoting centers (Fig. 4). It is thus pos-

sible that the MPA output inhibits wake-promoting neurons but also excites sleep-promoting neurons, whereas the DMH output might excite the former and inhibit the latter. Anatomically, MPA neurons contain various neuropeptides, such as galanin, gonadotropin-releasing hormone, and neurotensin, as well as GABA (Tohyama and Takatsuji, 1998), and these neurons may be functionally and hodologically different. In the DMH, neurons that projected to the sleep-related ventrolateral preoptic nucleus were predominantly GABAergic, whereas those projecting to the orexin field contained mainly glutamate or thyrotropin-releasing hormone (Chou et al., 2003). The projections from the SPVZ to the DMH were also segregated according to their functions (Chou et al., 2003), and it is possible that similar segregation exists for the projections, shown in the present study, from the SPVZ to the orexin field, tuberomammillary nucleus and the sleep-promoting preoptic nuclei.

These available data support the possibility that the MPA might relay the circadian signal generally to inhibit wakefulness, whereas the DMH might do so to enhance it, and that in each of the three proposed relay nuclei, different neurons might mediate the circadian signal to sleep- and wake-promoting cell groups. The segregation of the pathways might even start within the SCN as demonstrated anatomically (Moore and Leak, 2001; Buijs et al., 2003) and suggested physiologically (Hermes et al., 1996; Kalsbeek and Buijs, 1996; Sun et al., 2000, 2001; Cui et al., 1997). The differential distribution of endogenously rhythmic and light-responsive cells in the core and shell region of the SCN (Hamada et al., 2001; Lee et al., 2003) and their contributions to SCN efferent pathways (Kriegsfeld et al., 2004) suggest that the MPA, SPVZ and DMH may receive different amounts of information regarding photic input and oscillatory status, and, in turn, relay such signals differentially to neuronal systems controlling wake, non-REM and REM sleep.

CONCLUSIONS

Based on the present anatomical findings, together with the results of previous anatomical and functional studies, we propose that the SPVZ, DMH and MPA may stand as an interface between the SCN on one hand, and diverse physiological systems including the sleep–wake system, on the other. In addition to humoral factors that are thought to mediate the circadian signal from the SCN (see introduction), these multiple indirect as well as direct synaptic pathways may provide routes by which the SCN can modulate the activity pattern of various neuronal networks, including those controlling sleep and wakefulness, allowing appropriate timing of their activation according to the time of day. We have previously discussed the advantages of indirect pathways, including the amplification of the circadian signal and the integration of the circadian message with other information (see Deurveilher et al., 2002). These features are likely to enhance the flexibility and adaptability of physiological and behavioral responses to internal and external signals. One such example is an alteration in daily sleep–wake cycles in response to changes in internal (e.g. homeostatic sleep drive, hormonal status) and external milieux (e.g. food availability, competition for habitat, time change). Finally, the neuronal connections between the SCN and the sleep/wake-related structures are not unidirectional but reciprocal (Bina et al., 1993; Deboer et al., 2003). These reciprocal interactions between the circadian timing and sleep–wake-regulatory systems may ensure the stable yet adaptive rhythmicity of daily cycles of sleep and wakefulness.

Acknowledgments—We thank Ms Joan Burns for excellent technical assistance and Dr. Hugh Piggins for helpful comments on an early version of the manuscript. This work was supported by the Canadian Institutes of Health Research (MOP-42553), and the Province of Nova Scotia Department of Health. S.D. was supported by postdoctoral fellowships from the Fondation Singer-Polignac and the Nova Scotia Health Research Foundation.

REFERENCES

Abe H, Honma S, Ohtsu H, Honma K (2004) Circadian rhythms in behavior and clock gene expressions in the brain of mice lacking histidine decarboxylase. Brain Res Mol Brain Res 124:178–187.

Abrahamson EE, Leak RK, Moore RY (2000) The suprachiasmatic nucleus projects to posterior hypothalamic arousal systems. Neuroreport 12:435–440.

Asala SA, Okano Y, Honda K, Inoue S (1990) Effects of medial preoptic area lesions on sleep and wakefulness in unrestrained rats. Neurosci Lett 114:300–304.

Aston-Jones G, Chen S, Zhu Y, Oshinsky ML (2001) A neural circuit for circadian regulation of arousal. Nature 4:732–738.

Behbehani MM, Da Costa Gomez TM (1996) Properties of a projection pathway from the medial preoptic nucleus to the midbrain periaqueductal gray of the rat and its role in the regulation of cardiovascular function. Brain Res 740:141–150.

Bina KG, Rusak B, Semba K (1993) Localization of cholinergic neurons in the forebrain and brainstem that project to the suprachiasmatic nucleus of the hypothalamus in rat. J Comp Neurol 335:295–307.

Buijs RM, Kalsbeek A (2001) Hypothalamic integration of central and peripheral clocks. Nat Rev Neurosci 2:521–526.

Buijs RM, la Fleur SE, Wortel J, Van Heyningen C, Zuiddam L, Mettenleiter TC, Kalsbeek A, Nagai K, Niijima A (2003) The suprachiasmatic nucleus balances sympathetic and parasympathetic output to peripheral organs through separate preautonomic neurons. J Comp Neurol 464:36–48.

Cagampang F, Yamazaki S, Otori Y, Inouye S (1993) Serotonin in the raphe nuclei: regulation by light and an endogenous pacemaker. Neuroreport 5:49–52.

Cheng MY, Bullock CM, Li C, Lee AG, Bermak JC, Belluzzi J, Weaver DR, Leslie FM, Zhou QY (2002) Prokineticin 2 transmits the behavioural circadian rhythm of the suprachiasmatic nucleus. Nature 417:405–410.

Chiba T, Murata Y (1985) Afferent and efferent connections of the medial preoptic area in the rat: a WGA-HRP study. Brain Res Bull 14:261–272.

Chou TC, Bjorkum AA, Gaus SE, Lu J, Scammell TE, Saper CB (2002) Afferents to the ventrolateral preoptic nucleus. J Neurosci 22:977–990.

Chou TC, Scammell TE, Gooley JJ, Gaus SE, Saper C, Lu J (2003) Critical role of dorsomedial hypothalamic nucleus in a wide range of behavioral circadian rhythms. J Neurosci 23:10691–10702.

Coolen LM, Wood RI (1998) Bidirectional connections of the medial amygdaloid nucleus in the Syrian hamster brain: simultaneous

anterograde and retrograde tract tracing. J Comp Neurol 399:189–209.
Coolen LM, Jansen HT, Goodman RL, Wood RI, Lehman MN (1999) A new method for simultaneous demonstration of anterograde and retrograde connections in the brain: co-injections of biotinylated dextran amine and the beta subunit of cholera toxin. J Neurosci Methods 91:1–8.
Cui LN, Saeb-Parsy K, Dyball RE (1997) Neurones in the supraoptic nucleus of the rat are regulated by a projection from the suprachiasmatic nucleus. J Physiol 502:149–159.
Deboer T, Vansteensel MJ, Detari L, Meijer JH (2003) Sleep states alter activity of suprachiasmatic nucleus neurons. Nat Neurosci 6:1086–1090.
Deurveilher S, Semba K (2003) Indirect projections from the suprachiasmatic nucleus to the median preoptic nucleus in rat. Brain Res 987:100–106.
Deurveilher S, Hars B, Hennevin E (1997) Pontine microinjection of carbachol does not reliably enhance paradoxical sleep in rats. Sleep 20:593–607.
Deurveilher S, Burns J, Semba K(2001a) Indirect pathways from the suprachiasmatic nucleus to hypocretin/orexin-containing, monoaminergic and cholinergic cell groups in rat. Soc Neurosci Abstr 27:410.5.
Deurveilher S, Burns J, Semba K (2001b) Indirect projections from the suprachiasmatic nucleus to wake-related neuronal groups in the forebrain and brainstem in rat. Sleep Suppl 24:A135
Deurveilher S, Burns J, Semba K (2001c) Anatomical analysis of indirect efferent pathways of the suprachiasmatic nucleus to wake-related cell groups in rat. Actas de Fisiología 7:132
Deurveilher S, Burns J, Semba K (2002) Indirect projections from the suprachiasmatic nucleus to the ventrolateral preoptic nucleus: a dual tract-tracing study in rat. Eur J Neurosci 16:1195–1213.
Ericson H, Blomqvist A, Kohler C (1991) Origin of neuronal inputs to the region of the tuberomammillary nucleus of the rat brain. J Comp Neurol 311:45–64.
Estabrooke IV, McCarthy MT, Ko E, Chou TC, Chemelli RM, Yanagisawa M, Saper CB, Scammell TE (2001) Fos expression in orexin neurons varies with behavioral state. J Neurosci 21:1656–1662.
Fahrbach SE, Morrell JI, Pfaff DW (1986) Identification of medial preoptic neurons that concentrate estradiol and project to the midbrain in the rat. J Comp Neurol 247:364–382.
Feenstra MG, Botterblom MH, Mastenbroek S (2000) Dopamine and noradrenaline efflux in the prefrontal cortex in the light and dark period: effects of novelty and handling and comparison to the nucleus accumbens. Neuroscience 100:741–748.
Gaus SE, Saper CB (2000) Circadian control of sleep: disynaptic connections from the suprachiasmatic nucleus to the ventrolateral preoptic nucleus. Soc Neurosci Abstr 26:757.5.
Gerashchenko D, Kohls MD, Greco M, Waleh NS, Salin-Pascual R, Kilduff TS, Lappi DA, Shiromani PJ (2001) Hypocretin-2-saporin lesions of the lateral hypothalamus produce narcoleptic-like sleep behavior in the rat. J Neurosci 21:7273–7283.
Gonzales M, Lu W, Aston-Jones G (2002) Role of noradrenergic locus coeruleus (LC) system in sleep and waking: circadian factors. Soc Neurosci Abstr 28:871.11.
Grove EA (1988) Neural associations of the substantia innominata in the rat: afferent connections. J Comp Neurol 277:315–346.
Hamada T, LeSauter J, Venuti JM, Silver R (2001) Expression of Period genes: rhythmic and nonrhythmic compartments of the suprachiasmatic nucleus pacemaker. J Neurosci 21:7742–7750.
Hara J, Beuckmann CT, Nambu T, Willie JT, Chemelli RM, Sinton CM, Sugiyama F, Yagami K, Goto K, Yanagisawa M, Sakurai T (2001) Genetic ablation of orexin neurons in mice results in narcolepsy, hypophagia, and obesity. Neuron 30:345–354.
Hermes ML, Coderre EM, Buijs RM, Renaud LP (1996) GABA and glutamate mediate rapid neurotransmission from suprachiasmatic nucleus to hypothalamic paraventricular nucleus in rat. J Physiol 496:749–757.
Ibuka N, Inouye S, Kawamura H (1977) Analysis of sleep–wakefulness rhythms in male rats after suprachiasmatic nucleus lesions and ocular enucleation. Brain Res 122:33–47.
Inouye ST, Kawamura H (1979) Persistence of circadian rhythmicity in a mammalian hypothalamic "island" containing the suprachiasmatic nucleus. Proc Natl Acad Sci USA 76:5962–5966.
Isobe Y, Nishino H (2001) Circadian rhythm of drinking and running-wheel activity in rats with 6-hydroxydopamine lesions of the ventral tegmental area. Brain Res 899:187–192.
Kalen P, Karlson M, Wiklund L (1985) Possible excitatory amino acid afferents to nucleus raphe dorsalis of the rat investigated with retrograde wheat germ agglutinin and D-[^{3}H]aspartate tracing. Brain Res 360:285–297.
Kalsbeek A, Buijs RM (1996) Rhythms of inhibitory and excitatory output from the circadian timing system as revealed by in vivo microdialysis. Prog Brain Res 111:273–293.
Kametani H, Kawamura H (1991) Circadian rhythm of cortical acetylcholine release as measured by in vivo microdialysis in freely moving rats. Neurosci Lett 132:263–266.
Kapas L, Obal F Jr, Book AA, Schweitzer JB, Wiley RG, Krueger JM (1996) The effects of immunolesions of nerve growth factor-receptive neurons by 192 IgG-saporin on sleep. Brain Res 712:53–59.
Ko EM, Estabrooke IV, McCarthy M, Scammell TE (2003) Wake-related activity of tuberomammillary neurons in rats. Brain Res 992:220–226.
Kramer A, Yang FC, Snodgrass P, Li X, Scammell TE, Davis FC, Weitz CJ (2001) Regulation of daily locomotor activity and sleep by hypothalamic EGF receptor signaling. Science 294:2511–2515.
Kriegsfeld LJ, Leak RK, Yackulic CB, LeSauter J, Silver R (2004) Organization of suprachiasmatic nucleus projections in Syrian hamsters (*Mesocricetus auratus*): an anterograde and retrograde analysis. J Comp Neurol 468:361–379.
Leak RK, Moore RY (2001) Topographic organization of suprachiasmatic nucleus projection neurons. J Comp Neurol 433:312–334.
Lee HS, Billings HJ, Lehman MN (2003) The suprachiasmatic nucleus: a clock of multiple components. J Biol Rhythms 18:435–449.
Lee Y, Arbogast LA, Voogt JL (1998) Semicircadian rhythms of c-Fos expression in several hypothalamic areas during pregnancy in the rat: relationship to prolactin secretion. Neuroendocrinology 67:83–93.
Legoratti-Sanchez MO, Guevara-Guzman R, Solano-Flores LP (1989) Electrophysiological evidences of a bidirectional communication between the locus coeruleus and the suprachiasmatic nucleus. Brain Res Bull 23:283–288.
LeSauter J, Silver R (1998) Output signals of the SCN. Chronobiol Int 15:535–550.
Lu J, Greco MA, Shiromani P, Saper CB (2000) Effect of lesions of the ventrolateral preoptic nucleus on NREM and REM sleep. J Neurosci 20:3830–3842.
Lu J, Zhang Y-H, Chou T, Gaus SE, Elmquist JK, Shiromani P, Saper CB (2001) Contrasting effects of ibotenate lesions of the paraventricular nucleus and subparaventricular zone on sleep-wake cycle and temperature regulation. J Neurosci 21:4864–4874.
Luppi P-H, Aston-Jones G, Akaoka H, Chouvet G, Jouvet M (1995) Afferent projections to the rat locus coeruleus demonstrated by retrograde and anterograde tracing with cholera-toxin B subunit and *Phaseolus vulgaris* leucoagglutinin. Neuroscience 65:119–160.
Lydic R, Baghdoyan HA (1999) Handbook of behavioural state control: cellular and molecular mechanisms. Boca Raton: CRC Press.
Martinez GS, Smale L, Nunez AA (2002) Diurnal and nocturnal rodents show rhythms in orexinergic neurons. Brain Res 955:1–7.
McGinty D, Szymusiak R (2001) Brain structures and mechanisms involved in the generation of NREM sleep: focus on the preoptic hypothalamus. Sleep Med Rev 5:323–342.
Methippara MM, Alam MN, Szymusiak R, McGinty D (2003) Preoptic area warming inhibits wake-active neurons in the perifornical lateral hypothalamus. Brain Res 960:165–173.

Mochizuki T, Yamatodani A, Okakura K, Horii A, Inagaki N, Wada H (1992) Circadian rhythm of histamine release from the hypothalamus of freely moving rats. Physiol Behav 51:391–394.

Moore RY, Leak RH (2001) Suprachiasmatic nucleus. In: Circadian clocks: handbook of behavioral neurobiology (Takahashi JS, Turek FW, Moore RY, eds), pp 141–179. New York: Kluwer Academic/ Plenum Publishers.

Mouret J, Coindet J (1980) Polygraphic evidence against a critical role of the raphe nuclei in sleep in the rat. Brain Res 186:273–287.

Novak CM, Nunez AA (2000) A sparse projection from the suprachiasmatic nucleus to the sleep active ventrolateral preoptic area in the rat. Neuroreport 11:93–96.

Nunez AA, Bult A, McElhinny TL, Smale L (1999) Daily rhythms of Fos expression in hypothalamic targets of the suprachiasmatic nucleus in diurnal and nocturnal rodents. J Biol Rhythms 14:300–306.

Pace-Schott EF, Hobson JA (2002) The neurobiology of sleep: genetics, cellular physiology and subcortical networks. Nat Rev Neurosci 3:591–605.

Parmentier R, Ohtsu H, Djebbara-Hannas Z, Valatx JL, Watanabe T, Lin JS (2002) Anatomical, physiological, and pharmacological characteristics of histidine decarboxylase knock-out mice: evidence for the role of brain histamine in behavioral and sleep–wake control. J Neurosci 22:7695–7711.

Paulson PE, Robinson TE (1994) Relationship between circadian changes in spontaneous motor activity and dorsal versus ventral striatal dopamine neurotransmission assessed with on-line microdialysis. Behav Neurosci 108:624–635.

Paxinos G, Watson P (1998) The rat brain in stereotaxic coordinates. 4th edition. San Diego: Academic Press.

Peng ZC, Bentivoglio M (2004) The thalamic paraventricular nucleus relays information from the suprachiasmatic nucleus to the amygdala: a combined anterograde and retrograde tracing study in the rat at the light and electron microscopic levels. J Neurocytol 33:101–116.

Peterfi Z, Churchill L, Hajdu I, Obal F Jr, Krueger JM, Parducz A (2004) Fos-immunoreactivity in the hypothalamus: dependency on the diurnal rhythm, sleep, gender, and estrogen. Neuroscience 124:695–707.

Peyron C, Petit JM, Rampon C, Jouvet M, Luppi PH (1998) Forebrain afferents to the rat dorsal raphe nucleus demonstrated by retrograde and anterograde tracing methods. Neuroscience 82:443–468.

Prast H, Dietl H, Philippu A (1992) Pulsatile release of histamine in the hypothalamus of conscious rats. J Auton Nerv Syst 39:105–110.

Rizvi TA, Ennis M, Aston-Jones G, Jiang M, Liu W-L, Behbehani MM, Shipley MT (1994) Preoptic projections to Barrington's nucleus and the pericoerulear region: architecture and terminal organization. J Comp Neurol 347:1–24.

Rusak B, Zucker I (1979) Neural regulation of circadian rhythms. Physiol Rev 59:449–526.

Sakata M, Sei H, Toida K, Fujihara H, Urushihara R, Morita Y (2002) Mesolimbic dopaminergic system is involved in diurnal blood pressure regulation. Brain Res 928:194–201.

Saper CB, Chou TC, Scammell TE (2001) The sleep switch: hypothalamic control of sleep and wakefulness. Trends Neurosci 24:726–731.

Schwartz MD, Nunez AA, Smale L (2004) Differences in the suprachiasmatic nucleus and lower subparaventricular zone of diurnal and nocturnal rodents. Neuroscience 127:13–23.

Semba J, Toru M, Mataga N (1984) Twenty-four hour rhythms of norepinephrine and serotonin in nucleus suprachiasmaticus, raphe nuclei, and locus coeruleus in the rat. Sleep 7:211–218.

Semba K, Fibiger HC (1992) Afferent connections of the laterodorsal and the pedunculopontine tegmental nuclei in the rat: a retro- and antero-grade transport and immunohistochemical study. J Comp Neurol 323:387–410.

Simerly RB, Swanson LW (1988) Projections of the medial preoptic nucleus: a *Phaseolus vulgaris* leucoagglutinin anterograde tract-tracing study in the rat. J Comp Neurol 270:209–242.

Steininger TL, Gong H, McGinty D, Szymusiak R (2001) Subregional organization of preoptic area/anterior hypothalamic projections to arousal-related monoaminergic cell groups. J Comp Neurol 429:638–653.

Steriade M, McCarley RW (1990) Brainstem control of wakefulness and sleep. New-York: Plenum Press.

Sun X, Rusak B, Semba K (2000) Electrophysiology and pharmacology of projections from the suprachiasmatic nucleus to the ventromedial preoptic area in rat. Neuroscience 98:715–728.

Sun X, Whitefield S, Rusak B, Semba K (2001) Electrophysiological analysis of suprachiasmatic nucleus projections to the ventrolateral preoptic area in rat: implications for circadian control of behavioral state. Eur J Neurosci 14:1257–1274.

Swanson LW (1987) The hypothalamus. In: Handbook of chemical neuroanatomy: integrated systems of the CNS, part I: hypothalamus, hippocampus, amygdala, retina (Bjorklund T, Hokfelt T, Swanson LW, eds), pp 1–124. Amsterdam: Elsevier.

Szymusiak R, McGinty D (1989) Effects of basal forebrain stimulation on the waking discharge of neurons in the midbrain reticular formation of cats. Brain Res 498:355–359.

Taheri S, Sunter D, Dakin C, Moyes S, Seal L, Gardiner J, Rossi M, Ghatei M, Bloom S (2000) Diurnal variation in orexin A immunoreactivity and prepro-orexin mRNA in the rat central nervous system. Neurosci Lett 279:109–112.

ter Horst GJ, Luiten PG (1986) The projections of the dorsomedial hypothalamic nucleus in the rat. Brain Res Bull 16:231–248.

Thompson RH, Canteras NS, Swanson LW (1996) Organization of projections from the dorsomedial nucleus of the hypothalamus: a PHA-L study in the rat. J Comp Neurol 376:143–173.

Tohyama M, Takatsuji K (1998) Atlas of neuroactive substances and their receptors in the rat. Oxford: Oxford University Press.

Vrang N, Mikkelsen JD, Larsen PJ (1997) Direct link from the suprachiasmatic nucleus to hypothalamic neurons projecting to the spinal cord: a combined tracing study using cholera toxin subunit B and *Phaseolus vulgaris*-leucoagglutinin. Brain Res Bull 44:671–680.

Wainer BH, Mesulam MM (1990) Ascending cholinergic pathways in the rat brain. In: Brain cholinergic systems (Steriade M, Biesold D, eds), pp 65–119. Oxford: Oxford University Press.

Watts AG, Swanson LW (1987) Efferent projections of the suprachiasmatic nucleus: II. Studies using retrograde transport of fluorescent dyes and simultaneous peptide immunohistochemistry in the rat. J Comp Neurol 258:230–252.

Watts AG, Swanson LW, Sanchez-Watts G (1987) Efferent projections of the suprachiasmatic nucleus: I. Studies using anterograde transport of Phaseolus vulgaris leucoagglutinin in the rat. J Comp Neurol 258:204–229.

Wurts S, Edgar D (2000) Circadian and homeostatic control of rapid eye movement (REM) sleep: promotion of REM tendency by the suprachiasmatic nucleus. J Neurosci 20:4300–4310.

Yamatodani A, Mochizuki T, Mammoto T (1996) New vistas on histamine arousal hypothesis: microdialysis study. Methods Find Exp Clin Pharmacol 18(Suppl A):113–117.

Yoshida Y, Fujiki N, Nakajima T, Ripley B, Matsumura H, Yoneda H, Mignot E, Nishino S (2001) Fluctuation of extracellular hypocretin-1 (orexin A) levels in the rat in relation to the light-dark cycle and sleep-wake activities. Eur J Neurosci 14:1075–1081.

Zaretskaia MV, Zaretsky DV, Shekhar A, DiMicco JA (2002) Chemical stimulation of the dorsomedial hypothalamus evokes non-shivering thermogenesis in anesthetized rats. Brain Res 928:113–125.

Zeitzer JM, Buckmaster CL, Parker KJ, Hauck CM, Lyons DM, Mignot E (2003) Circadian and homeostatic regulation of hypocretin in a primate model: implications for the consolidation of wakefulness. J Neurosci 23:3555–3560.

Zhang S, Zeitzer JM, Yoshida Y, Wisor JP, Nishino S, Edgar DM, Mignot E (2004) Lesions of the suprachiasmatic nucleus eliminate the daily rhythm of hypocretin-1 release. Sleep 27:619–627.

(Accepted 17 August 2004)
(Available online 11 November 2004)